minerals

MDPI

Article

Structural Control on the Formation of Pb-Zn Deposits: An Example from the Pyrenean Axial Zone

Alexandre Cugerone [1,*], Emilien Oliot [1], Alain Chauvet [1], Jordi Gavaldà Bordes [2], Angèle Laurent [1], Elisabeth Le Goff [3] and Bénédicte Cenki-Tok [1]

1 Géosciences Montpellier, UMR CNRS 5243, Université de Montpellier, Place E. Bataillon, CC 60, 34095 Montpellier, France; emilien.oliot@umontpellier.fr (E.O.); alain.chauvet@umontpellier.fr (A.C.); angele.laurent@etu.umontpellier.fr (A.L.); benedicte.cenki-tok@umontpellier.fr (B.C.-T.)
2 Conselh Generau d'Aran, Vielha, 25530 Lleida, Spain; j.gavalda@aran.org
3 Bureau de Recherches Géologiques et Minières (BRGM), Territorial Direction Languedoc-Roussillon, 1039 Rue de Pinville, 34000 Montpellier, France; e.legoff@brgm.fr
* Correspondence: alexandre.cugerone@umontpellier.fr; Tel.: +33-643-983-585

Received: 21 September 2018; Accepted: 23 October 2018; Published: 26 October 2018

Abstract: Pb-Zn deposits and specifically Sedimentary-Exhalative (SEDEX) deposits are frequently found in deformed and/or metamorphosed geological terranes. Ore bodies structure is generally difficult to observe and its relationships to the regional structural framework is often lacking. In the Pyrenean Axial Zone (PAZ), the main Pb-Zn mineralizations are commonly considered as Ordovician SEDEX deposits in the literature. New structural field analyzes focusing on the relations between mineralization and regional structures allowed us to classify these Pb-Zn mineralizations into three types: (I) Type 1 corresponds to minor disseminated mineralization, probably syngenetic and from an exhalative source. (II) Type 2a is a stratabound mineralization, epigenetic and synchronous to the Variscan D_1 regional deformation event and (III) Type 2b is a vein mineralization, epigenetic and synchronous to the late Variscan D_2 regional deformation event. Structural control appears to be a key parameter in concentrating Pb-Zn in the PAZ, as mineralizations occur associated to fold hinges, cleavage, and/or faults. Here we show that the main exploited type 2a and type 2b Pb-Zn mineralizations are intimately controlled by Variscan tectonics. This study demonstrates the predominant role of structural study for unraveling the formation of Pb-Zn deposits especially in deformed/metamorphosed terranes.

Keywords: Pb-Zn deposits; Pyrenean Axial Zone; SEDEX; remobilization; structural control; sphalerite

1. Introduction

The world's most important Pb-Zn resources consist in Sedimentary-Exhalative (SEDEX) mineralizations [1]. These types of ore deposits are syngenetic sedimentary to diagenetic. Occurrence of laminated sulfides parallel to bedding associated to sedimentary features (graded beds, etc.) are the key geological argument [2]. These important deposits occur often in ancient metamorphosed and highly deformed terranes for example in Red Dog, Alaska [3,4]; Rampura, India [5]; or Broken Hill, Australia [6]. In these cases, the processes of ore formation are still largely debated. In consequence, unraveling the relationships between mineralization and orogenic remobilization(s) is essential in order to understand the genesis of Pb-Zn deposits in deformed and metamorphosed environments. For example, in Broken Hill [6–8] and Cannington [9] deposits in Australia some authors argued for a metamorphogenic and epigenetic mineralization as large metasomatic zones may have refined pre-existing Pb-Zn rich rocks. Other authors consider a pre-metamorphic and syngenetic origin with only limited remobilization linked to tectonic events [10–12]. In the world-class Jinding Pb-Zn deposit,

the host rock has undergone a complex tectonic deformation [13]. Some authors proposed a syngenetic origin of the deposit [14,15] whereas others argued for an epigenetic genesis of the deposit based on field study, textural evidences [16–19], fluid inclusion [19,20], and paleomagnetic age [13]. Nowadays, these high-tonnage Pb-Zn deposits are the preferential target of numerous academic and industrial studies also for the presence of rare metals like Ge, Ga, In, or Cd associated with sulfides.

The Pb-Zn deposits hosted in the Pyrenean Axial Zone (PAZ) area that has suffered Variscan tectonics [21–23] are usually considered to be SEDEX. As an example, due to their geometry and the presence of distal volcanic rocks, Bois et al. [24] and Pouit et al. [25] considered as SEDEX the Pb-Zn mineralizations located in the Pierrefitte anticlinorium. In Bentaillou area, Fert [26] and Pouit [27,28] demonstrated that the stratigraphic and sedimentary controls were dominant processes during the genesis of these mineralizations. In the Aran Valley, deposits (Liat, Victoria-Solitaria, and Margalida) have been studied by Pujals [29] and Cardellach et al. [30,31]. These authors concluded on a stratiform and possibly exhalative formation of Pb-Zn mineralizations associated with a poor remobilization during Variscan deformation. Only few authors have documented the impact of Variscan tectonics on the genesis of these mineralizations. These are Alonso [32] in Liat, Urets, and Horcalh deposits or Nicol [33] for Pierrefitte anticlinorium deposits. In the Benasque Pass area, south of the Bossòst anticlinorium, Garcia Sansegundo et al. [34] indicated probable Ordovician stratiform or stratabound Pb-Zn mineralizations intensely reworked during Variscan tectonics. The Pb isotopes study realized by Marcoux [35] showed a unique major event of Pb-Zn mineralization interpreted as sedimentary-controlled and Ordovician or Devonian in age. Remobilization processes of Pb isotopes seem however poorly constrained and a complete structural study related to these analyzes is lacking.

Pyrenean sulfide mineralizations are an excellent target for investigating the links between orogenic deformation(s) and the genesis of associated mineralization(s), as well as finding key arguments to make the distinction between strictly syngenetic or rather epigenetic mineralizations and structurally remobilized mineralizations. In this work we will demonstrate that Pb-Zn deposits from five districts in the PAZ, previously largely considered SEDEX, were actually formed through processes involving a strong structural control.

2. Geological Setting

The Pyrenean Axial Zone (PAZ, Figure 1) is the result of the collision between the Iberian and Eurasian plates since the Lower Cretaceous. Deep parts of the crust were exhumed during this orogeny. The PAZ is composed of Paleozoic metasedimentary rocks locally intruded by Ordovician granites deformed and metamorphosed during the Variscan orogeny, like the Aston or Canigou gneiss domes [23,36].

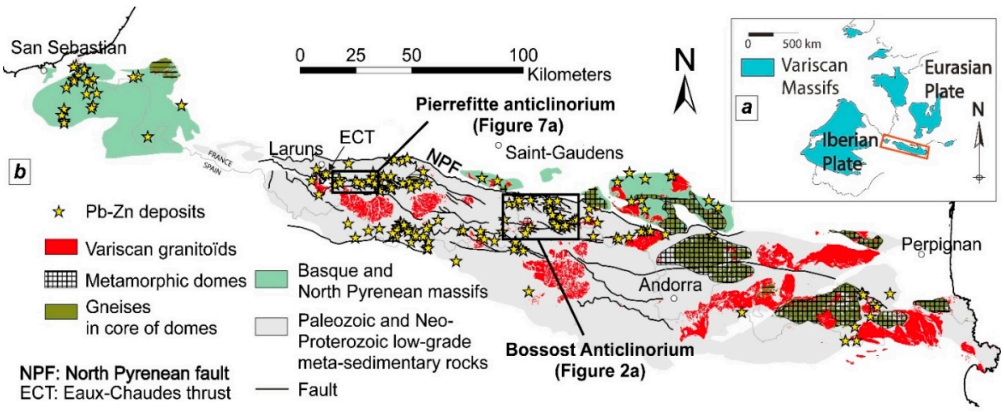

Figure 1. (**a**) Location of the Pyrenean Axial Zone (PAZ) within the Variscan belt of Western Europe. (**b**) Schematic map of the Pyrenean Axial Zone (PAZ) and location of all recognized Pb-Zn deposits (based on BRGM (French geological survey) and IGME (Spanish geological survey) databases). Note the abundance of these deposits especially in the central and western domains of the PAZ.

The PAZ is generally divided in two domains [21,36–39]: (i) a deep-seated domain called Infrastructure, which contains medium to high-grade metamorphic rocks and (ii) a shallow-seated domain called the Superstructure, which is composed of low-grade metamorphic rocks. The Infrastructure presents flat-lying foliations but highly deformed domains appear locally with steep and penetrative crenulation foliations. Alternatively, the Superstructure presents moderate deformation associated to a slaty cleavage [40,41] These two domains are intruded by Late-Carboniferous granites, like the Bossòst and the Lys-Caillaouas granites [37,42,43].

In the PAZ several deformation phases essentially Variscan in age (325–290 Ma) are recognized. The first deformation event (D_1) is marked by a cleavage (S_1) that is often parallel to the stratification (S_0). Regional M_1 metamorphism is of Medium-Pressure and Low-Temperature (MP/LT) and synchronous of this first D_1 deformation [22]. The second deformation event (D_2) is expressed by a moderate to steep axial planar (S_2) cleavage. M_2 is a Low-Pressure and High-Temperature (LP/HT) metamorphism linked to the Late-Variscan granitic intrusions, and it is superposed to the M_1 metamorphism [44,45]. Late-Variscan and/or Pyrenean-Alpine D_3 deformations are locally expressed as fold and shear zones like the Merens and/or probably the Bossòst faults [41,46,47].

The Pyrenean Pb-Zn regional district is the second largest in France with ~400,000 t Zn and ~180,000 t Pb extracted [48,49]. These sulfides deposits are localized in the PAZ in the Pierrefitte and Bossòst anticlinoriums (Figure 1b). Sphalerite (ZnS) and galena (PbS) are essentially present in Ordovician and Devonian metasediments. Few Pb-Zn deposits are hosted in granitic rocks [50].

This study focuses on Pb-Zn deposits located in the Bossòst anticlinorium (Figure 1) [42,44,51] and includes a comparison with Pb-Zn deposits occurring in the Pierrefitte anticlinorium. The southern part of the Bossòst anticlinorium forms the Aran Valley synclinorium. The northern part is limited by the North Pyrenean fault (Figure 2a). It is mostly composed of Cambrian to Devonian rocks and an intruding Late-Variscan leucocratic granite named the Bossòst granite.

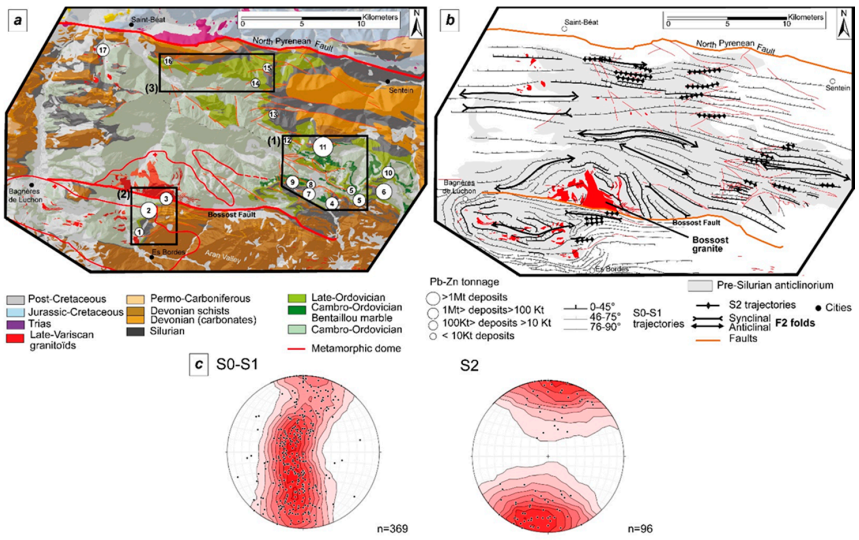

Figure 2. The Bossòst Anticlinorium. (**a**) Geological map with positions of the three districts: (1) Bentaillou-Liat-Urets district, see Figures 3 and 4; (2) Margalida-Victoria-Solitaria district, see Figure 5; and (3) Pale Bidau-Argut-Pale de Rase district, see Figure 6. Pb-Zn deposits are numbered as follows: 1: Solitaria; 2: Victoria; 3: Margalida; 4: Plan del Tor; 5: Urets; 6: Horcall; 7: Mauricio-Reparadora; 8: Estrella; 9: Liat; 10: Malh de Bolard; 11: Bentaillou; 12: Crabere; 13: Uls; 14: Pale Bidau; 15: Pale de Rase; 16: Argut. Lithologies are based on geological map of BRGM (France [52–54]) and IGME (Spain, Aran Valley; Garcia-Sansegundo et al. [55]). Metamorphic dome boundaries are related to andalousite isograd presented by Zwart; (**b**) Structural map with foliation trajectories of S_0-S_1, subvertical S_2, and related F_2 folds. Note preferential apparition of Pb-Zn deposits when S_2 cleavage is well-expressed. (**c**) Schmidt stereographic projections (lower hemisphere) of poles to S_0-S_1 and S_2 subvertical foliation planes.

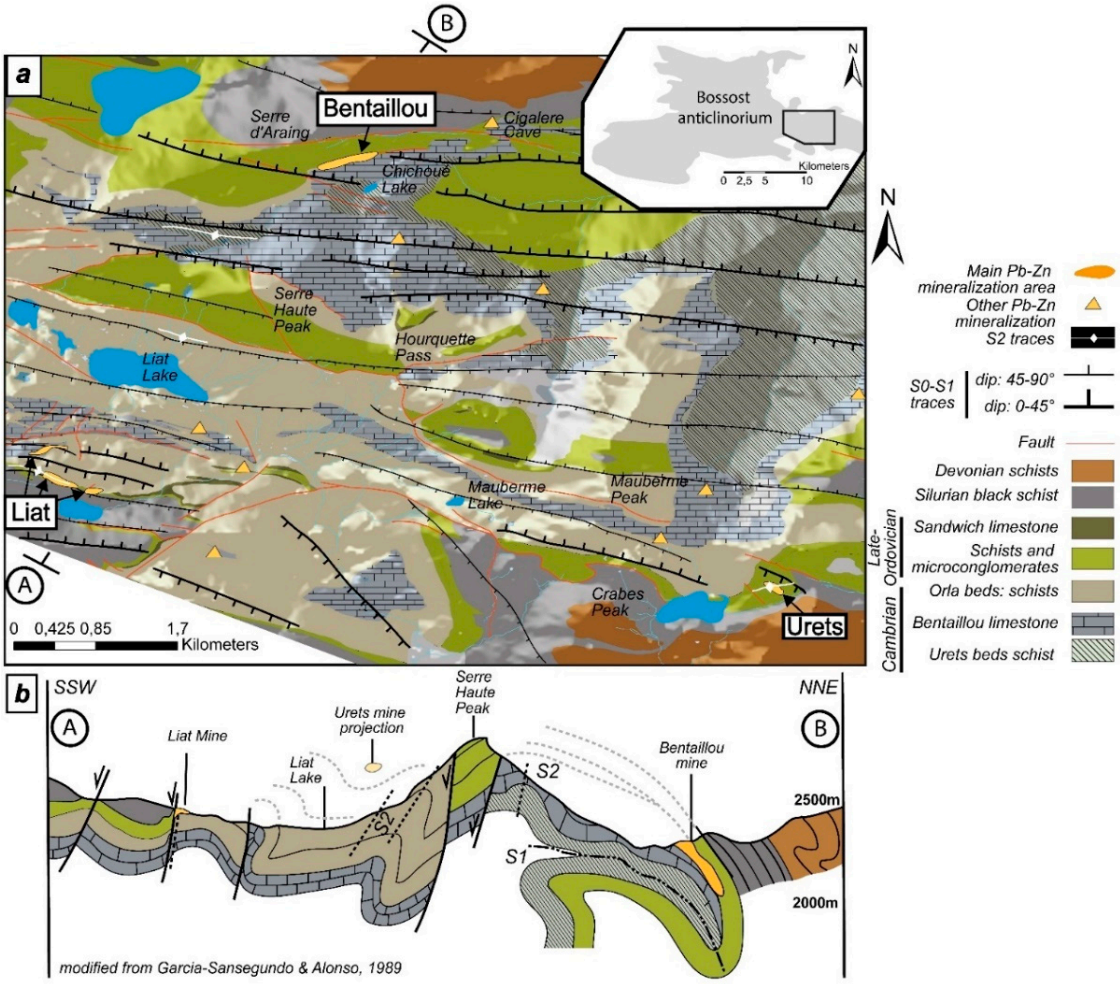

Figure 3. (**a**) Structural map of the Bentaillou-Liat-Urets district based on field study and BRGM/IGME geological maps. Location in Bossòst anticlinorium is indicated in the small sketch map (see also location on Figure 2a); (**b**) Structural NNE-SSW cross-section of the Liat-Bentaillou area. Location of the cross-section is indicated in the Figure 3a (modified from Garcia-Sansegundo and Alonso [56]). Note presence of Pb-Zn mineralization at rock competence interface and close to F1 fold hinge in Bentaillou mine.

Three main Pb-Zn districts are recognized in the Bossòst anticlinorium (Figure 2): (I) The Bentaillou-Liat-Urets district is located in the eastern part of the anticlinorium and was the most productive in the Bossòst anticlinorium, ~1.4 Mt at 9% of Zn and 2% of Pb metals [32,33]. (II) The Margalida-Victoria-Solitaria district is located in the southern part of the anticlinorium, close to the Bossòst granite. Production reached ~555,000 t with 11% Zn and 0.1% Pb [49]. (III) The Pale Bidau-Argut-Pale de Rase district is located in the northern part of the anticlinorium. Pb-Zn production did not exceed ~7000 t of Zn and ~3000 t of Pb [57].

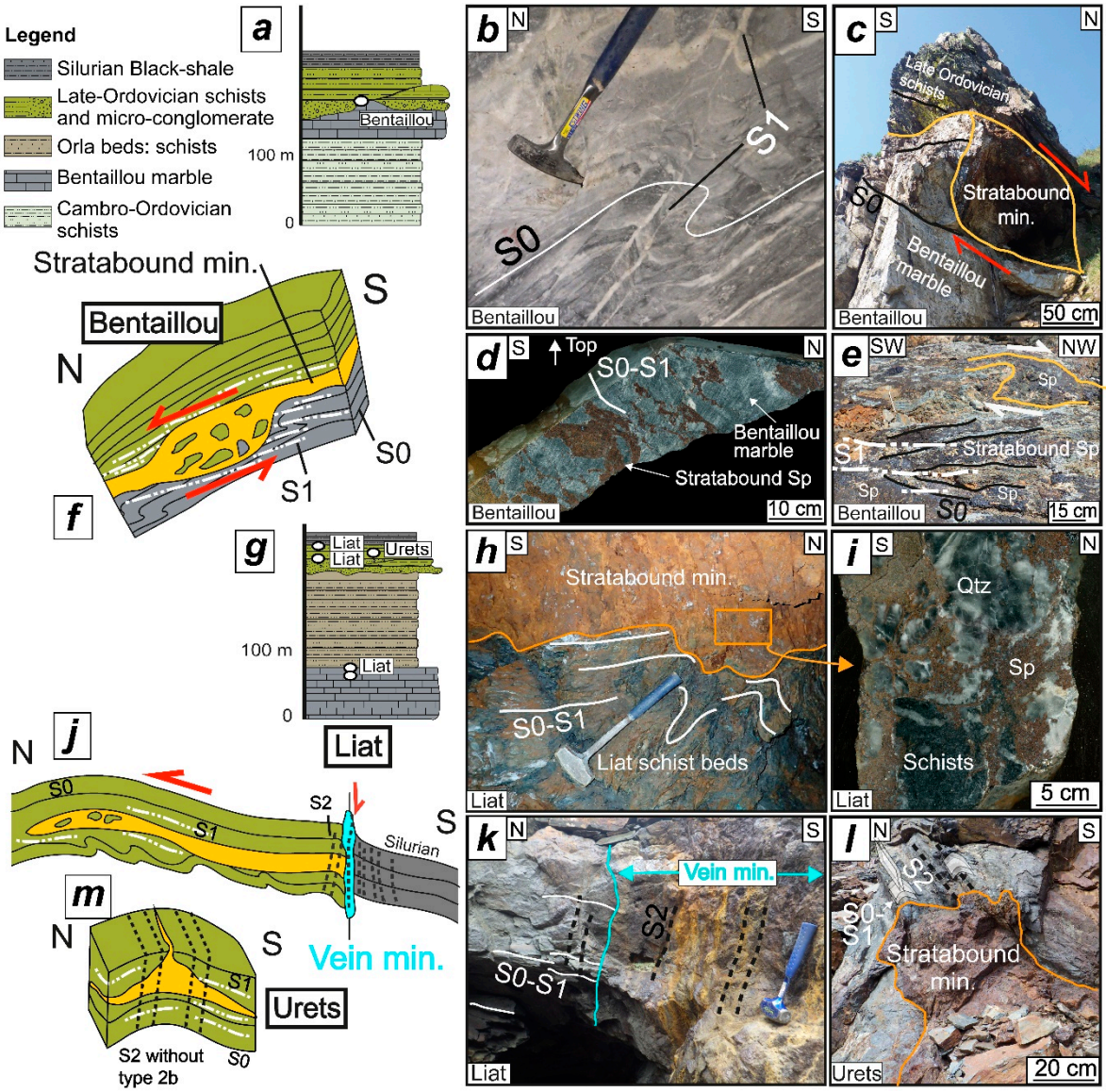

Figure 4. Field observation and structural models in the Bentaillou-Liat-Urets deposits (see location in Figure 3a). (**a**) Stratigraphic log of Bentaillou areas with position of the Pb-Zn deposits; (**b**) F_1 fold in Bentaillou marble with S_1 cleavage marked by calcite recrystallization; (**c**) pull-apart geometry of Pb-Zn mineralization in Bentaillou area; (**d**) oriented sample of typical mineralization in Bentaillou marble; and (**e**) relationship between sphalerite mineralization and host rock structure. Note that sphalerite is not folded by F_1 folds and intersect S0 stratification; (**f**) 3D structural model of Bentaillou deposits with Pb-Zn mineralization in cm to pluri-m pull apart geometry; (**g**) stratigraphic log of Liat-Urets area with position of the Pb-Zn deposits; (**h**) stratabound mineralization in top of folded schist beds in Liat area; (**i**) brecciated Pb-Zn mineralization in Liat area with clast of schist and quartz in sphalerite matrix; (**j**) 3D structural model of Liat deposit with dm to m stratabound and vein mineralizations; (**k**) vein Pb-Zn mineralization in Liat deposit; (**l**) stratabound mineralization in F_2 fold hinge in Urets deposit; (**m**) 3D structural model of Urets deposit with pluri-dm to m Pb-Zn mineralization in F_2 fold hinge. Mineral abbreviations: Qtz-quartz; Sp-sphalerite.

Pierrefitte anticlinorium is located north of the Cauteret granite and intersected by the Eaux-Chaudes thrust (ECT; Figure 1). It is essentially composed of Ordovician rocks in the West and Devonian terranes in the East. Two districts are studied: (I) Pierrefitte mines is the largest district in the PAZ which produced ~180,000 t of Zn, ~100,000 t of Pb and ~150 t of Ag [48]. (II) Arre and Anglas mines are located west to Pierrefitte mines. Pb-Zn production did not exceed ~6500 t of Zn [48].

3. Structural Analysis of Three Pb-Zn Districts in the Bossòst Anticlinorium

The Bossòst anticlinorium is a 30 × 20 km E-W-trending asymmetric antiform hosting a metamorphic dome (Figure 2a). Pre-Silurian lithologies are dominated by Cambro-Ordovician schists. Locally, other lithologies are present like the Cambro-Ordovician Bentaillou marble or the late-Ordovician microconglomerate and limestone (Figure 2b).

Two distinct cleavages can be observed in the Bossòst anticlinorium. S_1 transposes the S_0 stratification and is roughly oriented N090–N120°E with varied dip angles both to the north and to the south (Figure 2b,c). S_0-S_1 dip angles are low in the metamorphic dome (Figure 2b) but this pattern is not restricted to the core of the anticlinorium. In the eastern part of the anticlinorium, foliation is generally low to moderately dipping (0–45° N or S, Figure 2b) and Garcia-Sansegundo and Alonso [54] supposed the presence of large recumbent F_1 folds in the Bentaillou and Horcalh-Malh de Bolard areas. The presence of a Late Ordovician microconglomerate at the base of Bentaillou limestone is described by Garcia-Sansegundo and Alonso [56] and confirms this hypothesis. Furthermore, the presence of these folds is inferred by the observation of dm- to pluri-m north-verging recumbent F_1 folds in Bentaillou marble in the underground levels of the mine and also by their presence in the Devonian schists.

Close to the southern boundary of the Bossòst granite, S_0-S_1 foliation in high-grade schists is steeply dipping (Figure 2b). The S_2 cleavage trends N080–120°E and is generally sub-vertical (Figure 2c) as axial plane of F_2 south-verging folds. S_2 cleavage and related F_2 folds are particularly well developed in the southern part of the Bossòst anticlinorium (Figure 2b).

In the PAZ districts, three Pb-Zn mineralization types are commonly observed and two of these will be described below: Stratabound mineralization is subparallel to S_0-S_1 and Vein mineralization is parallel to S_2. Disseminated mineralization is not a key mineralization type and is spread in the host rocks.

3.1. District of Bentaillou-Liat-Urets

This district is located in the southeastern part of the Bossòst anticlinorium. Three main extraction areas are present in this district: (i) Bentaillou mine is located in the north of the district (Figure 3a). Exploitation finished in 1953 and produced ~110,000 t of Zn and ~40,000 t of Pb. At that time, it was the second largest mine in the Pyrenees [58], (ii) the Liat mine lays southwest of the district and (iii) Urets is located southeast of the district (Figure 3a). Both produced ~60,000 t of Zn [49]. Mineralization occurrences will be described in the following parts.

3.1.1. Bentaillou Area

Mineralization lays close to the hinge of a N090–110°E kilometer-size F_1 recumbent fold (Figure 3b) and is essentially located at the top of the Cambro-Ordovician marble, below the Late-Ordovician schists (Figure 4a). Mineralized stratabound bodies are broadly parallel to S_0-S_1 which is sub horizontal with a progressive increase of the dip from 45°N to 80°N to the lowest underground mine levels in the north (Figure 3b). Relicts axial planar S_1 of F_1 recumbent isoclinal folds are locally underlined by recrystallized calcite in N090–100°E axial planes (Figure 4b).

Pb-Zn stratabound mineralizations are present in cm- to pluri-m N-S open-filling structures which can be assimilated to pull-apart features (Figure 4c) that were formed in association with a dextral top to the north kinematic. These mineralized bodies show typical impregnation textures (Figure 4d) and sphalerite presents mm to cm grain sizes. Pb-Zn mineralization is absent in weakly D_1 deformed areas whereas it occurs in highly deformed domains associated to the appearance of S_1 cleavage in F_1 fold hinges (Figure 4e,f).

3.1.2. Liat Area

Pb-Zn mineralization is located at the rock interface (Figure 4g) and can be hosted in Bentaillou marble, especially on top of the marble, between the microconglomerate and Liat beds or between

Liat beds and the Silurian black-shale. The large hm-size open F_2 fold is bordered to the south by a Silurian synclinorium (Figure 3a,b). S_1 cleavage is strictly parallel to S_0 in the area. D_2 deformation is well expressed in the south at the contact between Silurian black-shale and Late Ordovician schists.

Mineralized stratabound bodies with pluri-dm to m-thickness appear parallel to the shallow dipping S_0-S_1. Folds in Liat schists are present locally at the base of the mineralization (Figure 4h). It presents a brecciated texture (Figure 4i) with clasts of quartz and schists. Sphalerite presents cm grain sizes. At the contact with the Silurian black-shale the dip of Late Ordovician schist increases and a normal fault is inferred. Vertical Pb-Zn vein mineralization parallel to S_2 is present in this fault. It intersects S_0 stratification, S_1 cleavage as well as stratabound mineralizations (Figure 4j,k). Vein mineralization also presents a brecciated texture and sulfide grains are oriented parallel to S_2. Sphalerite presents an infra-mm grain size.

3.1.3. Urets Area

This Pb-Zn mineralization is hosted in Liat schist. D_2 deformation is intensively present in this area, with numerous N100–130°E F_2 open to isoclinal folds associated to a subvertical N90–120°E S_2 cleavage. Stratabound pluri-dm to m Pb-Zn mineralization is mainly located in F_2 fold hinges (Figure 4l) and can locally intersect S_0 stratification (Figure 4m). Pb-Zn mineralization has a brecciated texture with mm sphalerite grains and mm to cm quartz clasts.

3.2. District of Margalida-Victoria-Solitaria

This district is located south of the Bossòst anticlinorium (Figure 2a). Three main extraction areas are present in this district from north to the south (Figure 5a): (i) Margalida mine is located close to the Bossòst granite next to the Bossòst fault, (ii) Victoria mine, and (iii) Solitaria mine lays south of the granite and north and west to Arres village. Margalida and Solitaria mine produced less than 50,000 t of ore with ~10% of Zn and 1% of Pb [49]. Victoria produced ~504,000 t with 11% of Zn and 1% of Pb [49].

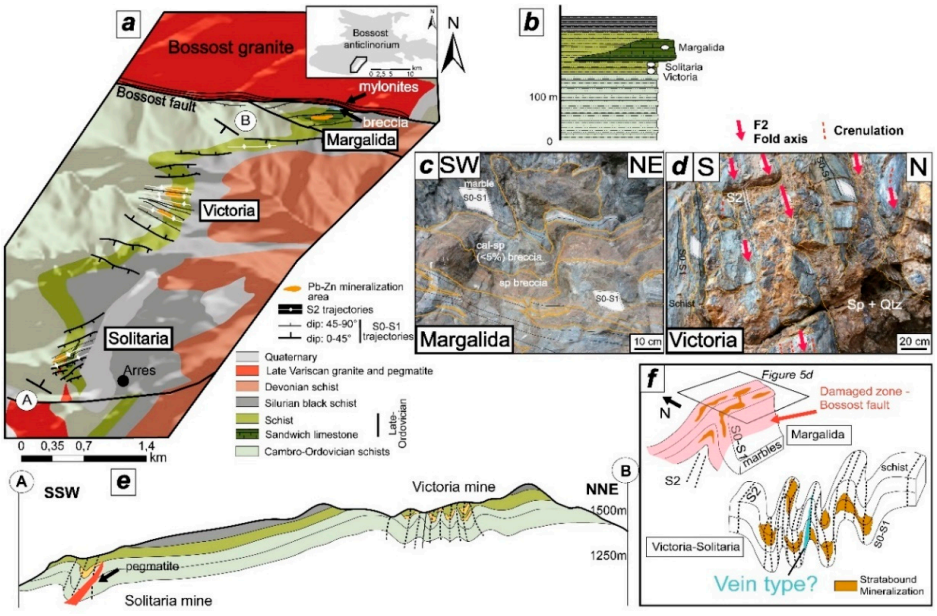

Figure 5. Margalida-Victoria-Solitaria district (see location on Figure 2a). (**a**) Structural map (lithologies are based on IGME geological map (Spain, Aran Valley; Garcia-Sansegundo et al. [1]) and location on the Bossòst anticlinorium (pre-Silurian rocks); (**b**) stratigraphic log; (**c**) stratabound Pb-Zn mineralization in Margalida mine hosted in Sandwich limestone level; (**d**) typical stratabound folded mineralization (F_2 isoclinal folds) in Victoria; (**e**) structural NNE-SSW cross-section of Victoria-Solitaria area; and (**f**) structural model of Margalida and Victoria-Solitaria mines. Mineral abbreviations: Cal—Calcite; Qtz—Quartz; Sp—Sphalerite.

3.2.1. Margalida Area

Pb-Zn mineralization is located in Late-Ordovician sandwich limestone (Figure 5a,b) which forms the core of an anticlinal presenting a vertical N100°E-trending axial plane (supposed F_2 fold). Mineralization is located in the damaged zone of the Bossòst N090°E-trending fault. Mineralization appears as pluri-dm lenses generally parallel to S_0-S_1. Still mineralization is not always concordant to S_0-S_1 (Figure 5c). The texture of sulfide mineralization in Margalida area is different to this in Victoria-Solitaria area as sulfide grain size is infra-mm.

3.2.2. Victoria-Solitaria Areas

Pb-Zn mineralization is hosted by Late Ordovician schists (Figure 5a,b,d) and generally parallel to S_0-S_1. Locally S_0-S_1 is intensively folded by F_2 asymmetrical isoclinal N090–N120°E folds and a vertical S_2 N070–110°E axial planar cleavage can be observed. Stratabound mineralization appears only in domains where F_2 folds imprint is intense (Figure 5e). Furthermore, in Victoria and Solitaria mines exploitation was preferentially undertaken in F_2 fold hinges. Pb-Zn mineralization is thicker in fold hinge (dm to m in thickness) and probably reworked during this D_2 deformation phase (Figure 5e,f). Sphalerite grains are often sub-millimetric. The presence of vein mineralization cannot be completely excluded as vertical galleries are present.

3.3. District of Pale Bidau-Argut-Pale de Rase

The general structural description of the district is given in [53]. In this section more details are given on the structural features of the Pale Bidau area (see location on Figure 2a).

Two different Pb-Zn mineralization geometries appear: a first stratabound mineralization is hosted only in F_2 fold pelitic level and concordant to S_0-S_1, marked by cm to pluri-m box-work texture. The second mineralization consists of veins oriented N090–120°E and consists of dm to m veins largely developed when D_2 deformation is important. Various dips are present for this mineralization but is mainly subvertical. Geometry of this mineralization can be interpreted as a pull-apart (Figure 6a) opened in a dextral top to the north movement and controlled by S_2 cleavage. Where S_2 cleavage is less pronounced, mineralization is thinner and seems to present in the sub-horizontal to 45°N S_0-S_1 cleavage (Figure 6b,c). Sphalerite crystals did not reach mm grain size.

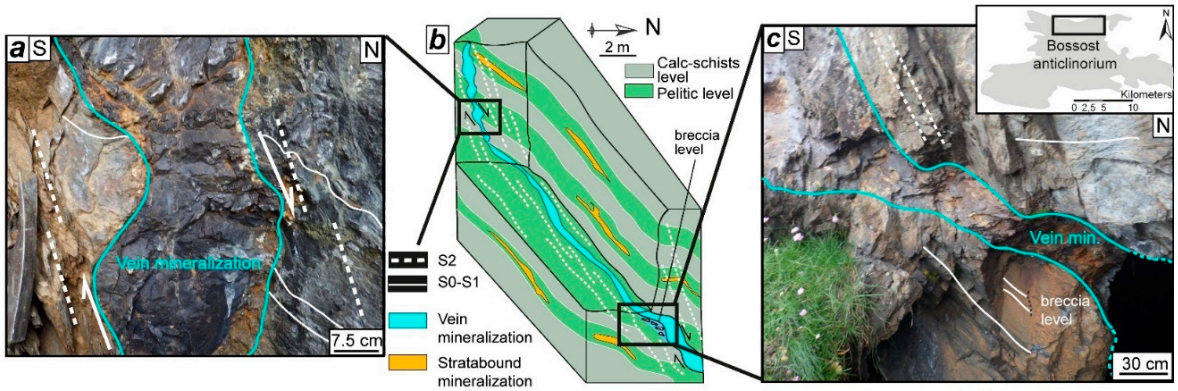

Figure 6. Field observations and 3D structural model of Pale Bidau deposit (see location in Figure 2a). (**a**) Vein Pb-Zn mineralization that occurs in pull-apart geometry; (**b**) 3D model presenting the relations between stratabound and vein Pb-Zn mineralizations; and (**c**) vein mineralization with presence of breccia at the base of a pull-apart mineralized structure.

4. Comparison with the Pierrefitte Anticlinorium: Pierrefitte and Arre-Anglas-Uzious Districts

The Pierrefitte anticlinorium is a 25 × 10 km NNW-SSE anticlinorium located in the western part of the PAZ (Figures 1b and 7a). Its core is composed of Ordovician schists and Late-Ordovician carbonated breccias. Upper stratigraphic levels are made of Silurian black-shales and Devonian rocks.

In western parts km-scale Valentin NNW-SSE anticlinal is included in the Pierrefitte anticlinorium. Compared to the Bossòst anticlinorium, the volume of late-Variscan granite or pegmatitic rocks outcropping is smaller and there is no metamorphic dome in the core (Figure 7a).

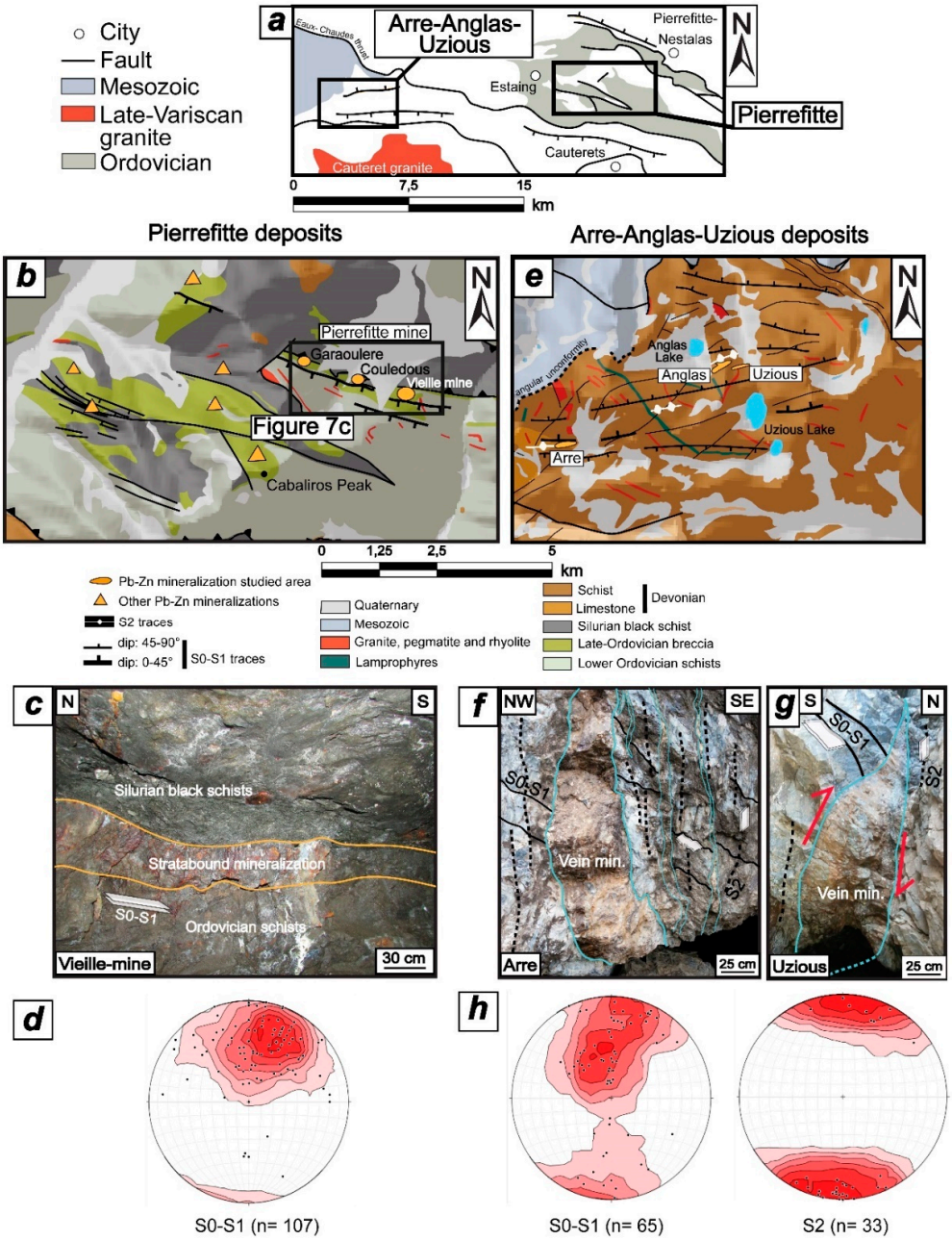

Figure 7. The Pierrefitte anticlinorium. (**a**) Simplified structural map showing the location of (**b**,**e**); (**b**) structural map zoomed on Pierrefitte mine (Lithologies are based on BRGM geological maps [59]; (**c**) photograph of typical stratabound Pb-Zn mineralization in Pierrefitte mine; (**d**) Schmidt stereographic projections (lower hemisphere) of poles to S_0-S_1 foliations measured in the Pierrefitte anticlinorium; (**e**) structural map of the Pierrefitte-Valentin anticlinorium zoomed on Anglas-Uzious and Arre mines (Lithologies are based on BRGM geological maps); (**f**) photograph of Arre vein mineralization parallel to S_2 cleavage; (**g**) photograph of Anglas-Uzious vein mineralization; and (**h**) Schmidt stereographic projections (lower hemisphere) of poles to S_0-S_1 and S_2 foliations measured in Anglas-Uzious and Arre areas.

The Pierrefitte anticlinorium is structured by several thrusts within Silurian levels (Figure 7b,c) associated to D_1 deformation. S_2 vertical N090–100°E cleavage is well expressed in Devonian levels at the rim of the anticlinorium but is less visible in the Ordovician core.

Numerous Pb-Zn mines are present in Late-Ordovician and Devonian terranes. These have produced ~3 Mt (average 9% of Zn and 5% of Pb).

4.1. Pierrefitte District

The Pierrefitte mines (Garaoulere, Couledous, Vieille-Mine) are located at the contact with Late Ordovician rocks mainly carbonate breccia. N100–110°E S_0-S_1 foliation moderately dips (20° to 60°) to the south (Figure 7d).

Stratabound mineralization lays at the top of the Late Ordovician series at the contact or within the Silurian black-shales (Figure 7c), which follows a regional thrust parallel to S_0-S_1. The presence of a thrust in Pierrefitte area is reported in [21,60,61] and this observation is supported in galleries by the occurrence of dm-scale dextral shear bands with a top-to-the-north-east kinematic. The mine galleries and the main exploited ore follow this regional thrust zone. S_1 cleavage often transposed S_0 stratification and corresponds to axial planes of isoclinal recumbent F_1 N090–120°E folds.

4.2. Arre-Anglas-Uzious District

Arre and Anglas-Uzious mines are hosted by Devonian schists and Lower Devonian limestone respectively (Figure 7e). S_2 cleavage is well-expressed even in Devonian limestone in the area and subvertical with a N090–100°E trend.

Arre mine is located in the western hinge of the Pierrefitte anticlinorium close to the contact of limestone and schistose rocks. The mineralization is composed of two ore bodies showing a trend of N040–090°E and a dip of 70°N to 90°N. Mineralization appears parallel to S_2 cleavage and discordant to S_0-S_1 (Figure 7f) which is typical of a vein mineralization. Anglas and Uzious mines are located in the northern part of the Pierrefitte anticlinorium. Mineralization consists in multiple pluri-centimeters to m vein orebodies, with several orientations from N060° to N100°E and subvertical dips. Uzious veins intersect magmatic aplite with a N050°E trend and have a pull-apart geometry (Figure 7g) linked to the presence of N090–100°E S_2 weak structures (Figure 7h). Many conjugate fractures N030–50°E with various dips are filled with mineralization close to the veins but their extension is limited to few dm.

5. Ore Petrology and Microstructures

A synthetic paragenetic sequence of the three Pb-Zn mineralization geometries investigated in this study is presented in the Figure 8. Disseminated mineralization represents the primary layered ore that is essentially composed of sparsely disseminated pluri-μm to mm grains of sphalerite, pyrite, magnetite, and galena. In all the studied deposits this mineralization is minor and does not constitute the exploited ore. Sulfides may appear in graded-beds or have a typical framboidal appearance (Figure 9a).

Stratabound and vein mineralizations constitute the main sulfides mineralizations. Sphalerite is the more widespread sulfide in these two mineralizations. Pyrite, galena pyrrhotite, chalcopyrite, and arsenopyrite are present in minor amounts. Metamorphic muscovite, chlorite, or biotite are intimately associated to sulfide mineralization. In Victoria-Solitaria, metamorphic Zn-spinel or gahnite is present in the host rocks and in breccia clasts in stratabound sulfide mineralization. The presence of gahnite in Victoria was previously reported [62]. In the host rock gahnite is elongated parallel to S_1 and is intersected by stratabound mineralization (Figure 9b).

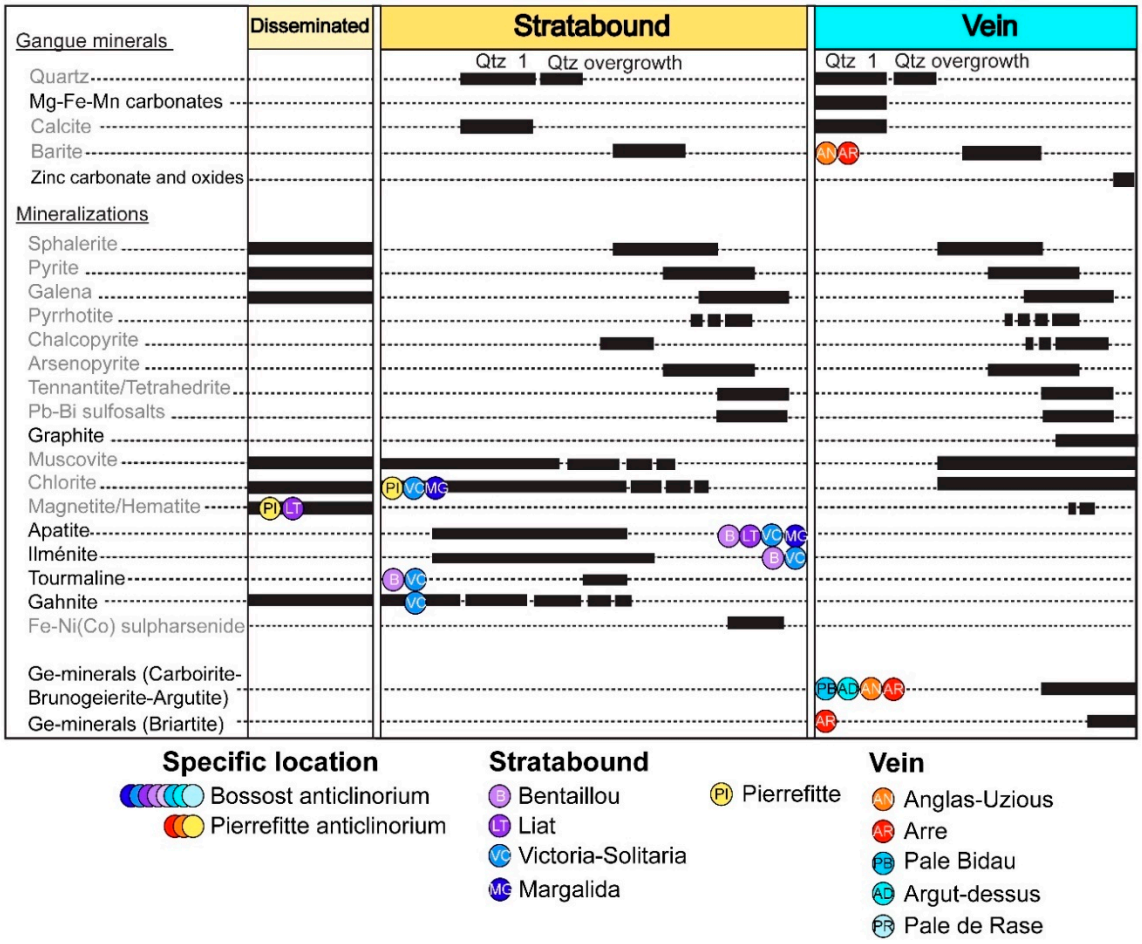

Figure 8. Paragenetic succession of ore and gangue minerals for all the eleven Pyrenean-studied Pb-Zn deposits. Minerals in grey are common to both stratabound and vein mineralizations and minerals in black are only present in stratabound or vein. Minerals only reported in a deposit are noted with the deposit circle. Several minerals like apatite, ilmenite, or tourmaline are only present in stratabound mineralization. Ge-minerals, graphite zinc carbonates or oxides, and Mg-Fe-Mn carbonates are only observed in vein mineralization (n = 110).

Stratabound Pb-Zn mineralization is a post-disseminated mineralization. SEM images show a primary framboidal galena intersected by a secondary stratabound pull-apart mineralization in the Bentaillou mine (Figure 9a).

In the Pierrefitte anticlinorium stratabound magnetite is abundant, especially in the Pierrefitte mine. It has crystallized prior to sphalerite. In the Pierrefitte mine syn-cinematic sphalerite crystallizes in asymmetric pressure shadows around a clast of magnetite (Figure 9c). Sphalerite appears parallel to S_1 cleavage and intersects S_0 stratification in an isoclinal F_1 fold hinge (Figure 9d). In the Bossòst anticlinorium and especially in Liat mine, sphalerite and quartz mineralization intersect F_2 folded pelitic rocks (Figure 9e). The same quartz associated to sphalerite is present in crack and seal veins (Figure 9e). In Margalida a typical durchbewegung texture with quartz spheroids in a sphalerite matrix shows a deformational imprint on this mineralization.

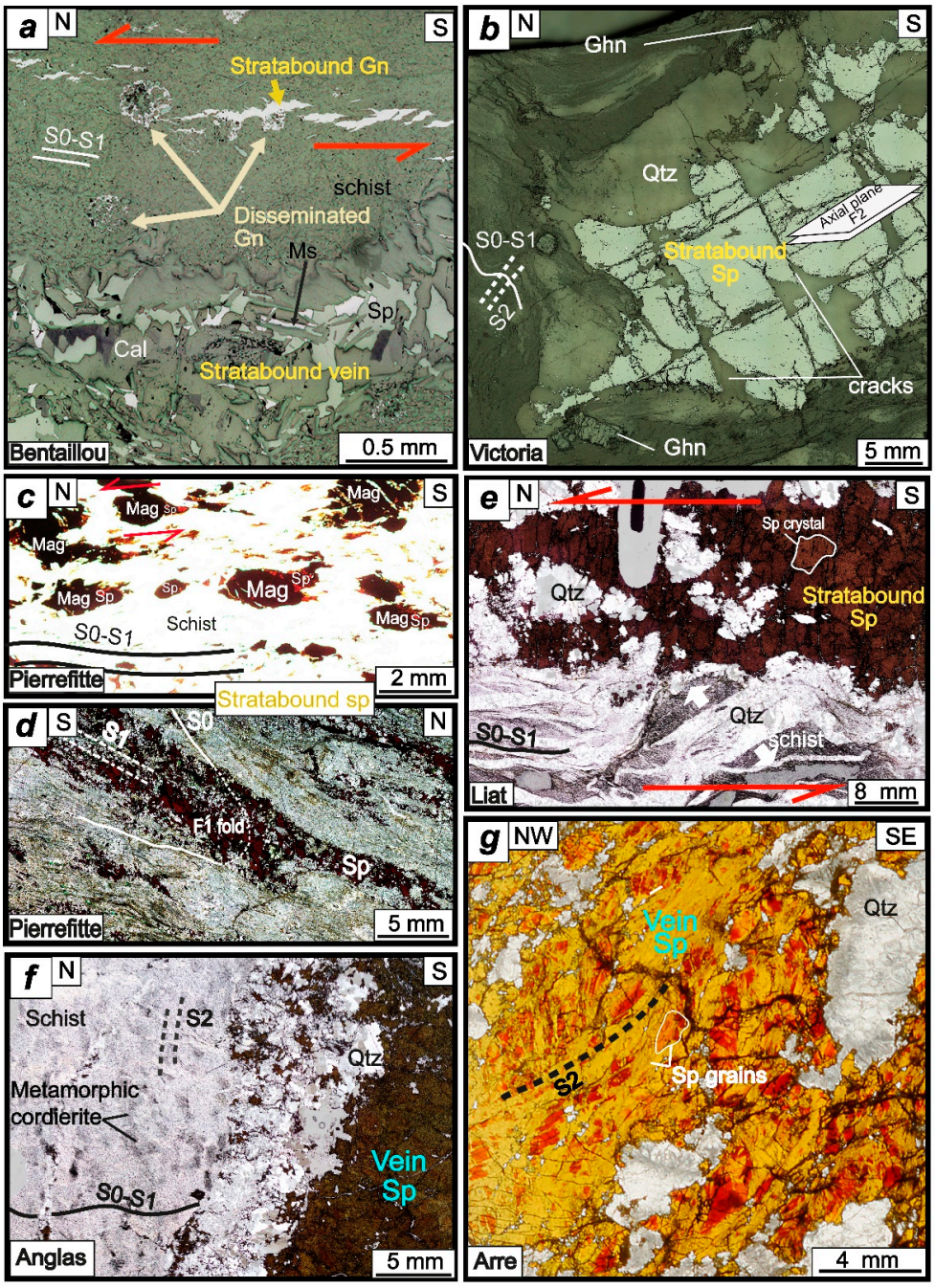

Figure 9. Microphotographs showing characteristics textures in the three mineralization types. (**a**) Bentaillou disseminated mineralization truncated by stratabound mineralizations (reflected light); (**b**) stratabound Victoria folded mineralization which intersects gahnite D_1 metamorphic mineral (reflected light); (**c**) syn-kinematic sphalerite which crystallizes in asymmetric pressure shadows around clasts of magnetite in Pierrefitte mine (transmitted light); (**d**) sphalerite mineralization from Pierrefitte mine parallel to S_1 and in F_1 isoclinal fold hinge. Mineralization intersects S0 stratification (transmitted light); and (**e**) stratabound sphalerite and quartz mineralizations which intersect pelitic host rock in Liat mine. Sphalerite is interpreted syn-kinematic D_1 (transmitted light); (**f**) vein mineralization in Anglas mine which intersect S_0-S_1 and parallel to S_2 cleavage marked by metamorphic cordierite (transmitted light); and (**g**) deformed and recrystallized vein sphalerite in Arre deposit. The two textures are identified with white line Recrystallization area in yellow marked S_2 cleavage (transmitted light). Mineral abbreviations: Cal—Calcite; Ghn—Gahnite; Gn—Galena; Mag—Magnetite; Ms—Muscovite; Qz—Quartz; Sp—Sphalerite.

Stratabound mineralization contain apatite, ilmenite, and tourmaline minerals that are only observed in this mineralization. In the Pierrefitte mineralization, the abundance of chlorite and muscovite associated to the mineralization is remarkable compared to other Pyrenean deposits.

Vein mineralization intersects S_0 at the micron scale (Figure 9f). In the Anglas deposit, vein mineralization is essentially composed of sphalerite, galena, quartz and calcite. The hanging wall of the vein is parallel to S_2 foliation and is marked by cordierite crystallization. Sphalerite in vein mineralization appears highly deformed and recrystallized with mm relictual grains and recrystallized µm-size crystals (like in Arre deposit, see Figure 9g). In Pale Bidau deposit, vein mineralization is only present in domains where the S_2 cleavage is well-marked. Note that Ge-minerals are exclusively present in the vein mineralization (Figure 8).

6. Discussion

6.1. Types of Pb-Zn Mineralizations in the PAZ

The presence of three major types of Pb-Zn mineralizations is demonstrated in this study: Disseminated but layered mineralization, which is now defined as Type 1, appears with graded-beds and framboidal appearance (Figure 9a). Stratabound mineralization (now defined as Type 2a) is a syn-D_1 mineralization concordant to the S_1 foliation. Vein mineralization (now defined as Type 2b) is a syn- to post-D_2 vein-type mineralization, parallel to the subvertical S_2 foliation. Type 2a and Type 2b are undoubtedly epigenetic and were formed as a consequence of Variscan tectonics.

The first and earlier Type 1 mineralization (Figure 10) is recognized in all the studied deposits in the Bossòst and Pierrefitte anticlinoriums, but it is not the main exploited resources. Its formation may be linked to the early volcanic Ordovician or Devonian events as proposed by Pouit [27] and Reyx [63]. In Pierrefitte anticlinorium, Nicol [55] proposed a unique Devonian source for the Pb-Zn mineralizations. Syngenetic formation is preferred for the Type 1 mineralization as sulfides appear layered and with sedimentary affinities. Nevertheless, framboidal texture may as well form in a post-sedimentation environment like in hydrothermal veins [64].

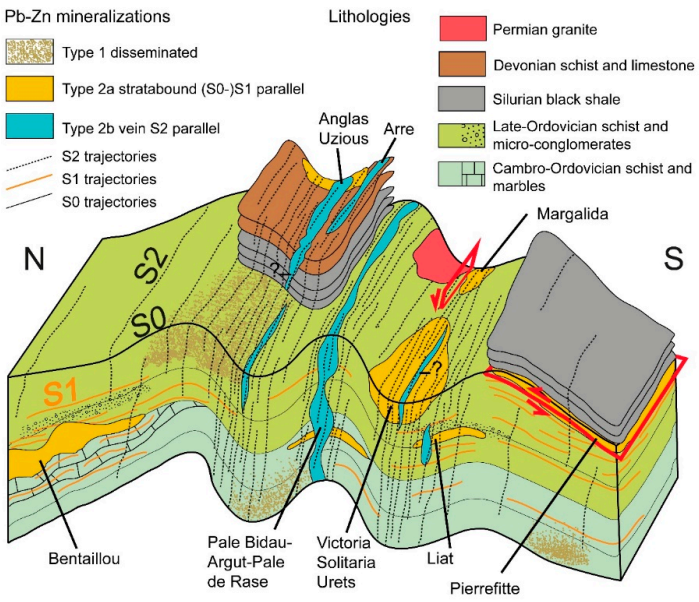

Figure 10. Schematic 3D sketch displaying the three main mineralization types which are typically observed in the studied area and related to each studied deposit. Note cm to pluri-m pull apart geometries in Bentaillou Type 2a mineralizations and in Type 2b mineralizations. Type 2b vein mineralizations are located in intensely S2 deformed domains. Other structural traps like saddle-reef formation in fold hinge or rock competence interfaces are represented for Victoria-Solitaria, Urets, Pierrefitte, and Liat deposits respectively.

The second stratabound Type 2a mineralization (Figure 10) is deposited parallel to S_0-S_1. It corresponds to the main Pb-Zn mineralization episode in the PAZ (~95% of the total exploited ore volume). In the Bentaillou area, Type 2a mineralization intersects S_0 stratification and is hosted by S_1 cleavage (Figure 4e), which is axial planar to isoclinal F_1 folds. Fert [26] and Pouit [27,28] proposed a syngenetic model for the Bentaillou deposit and described a normal stratigraphic succession that has been later folded by F_2 folds. F_1 isoclinal recumbent N090°E folds are absent in their model. Here we observe that Bentaillou Pb-Zn mineralization is localized essentially close to F_1 fold hinges at the interface between marble and schist or microconglomerate (Figure 4c). The source for Type 2a sulfides may be related to layered and supposed syngenetic Type 1 sulfides that are disseminated in the Ordovician and Devonian neighboring metasediments, or to Late-Variscan granitic intrusions, probably at least temporally close to the Type 2a mineralizations. Opening of top to the north cm to pluri-m pull-apart-type structures (Figure 4c) enables the formation of the large amount of mineralizations in Bentaillou. Pb-Zn ore is not observed at the base of Bentaillou marbles due to important karstification (Cigalere cave, Figure 3a), however it is deposed at Bularic [65] both above and below this marble level. In the Liat area, Pujals [29] described a syngenetic or diagenetic mineralization with apparent limited reworking. Our model shows that Type 2a stratabound mineralization is linked to the Variscan D_1 deformation. In the Victoria-Solitaria area, Type 2a stratabound mineralization occurs where D_2-related structures are present and can be locally remobilized in fold hinges. These thicker mineralizations in fold hinge may be linked to the saddle-reef process [66–68] associated with formation of the dilatation zone during folding. These deposits have been studied by Pujals [29], Cardellach et al. [30,69], Alvarez-Perez et al. [70], and Ovejero-Zappino [49,71]. These authors argued for a SEDEX origin based on syngenetic mineralization associated to the presence of syn-sedimentary faults. These models differ from our hypothesis: here we report that S_1 cleavage is parallel to axial plane of recumbent km-size isoclinal folds and transposes the S_0 stratification. F_2 folded Type 2a stratabound mineralization is thicker in fold hinge and intersects metamorphic minerals as gahnite. Presence of this Zn-spinel may be linked to a primary minor sulfide mineralization (Type 1, Figure 10) or to a D_1 metamorphic fluid rich in Zn. Chemistry of gahnite was analyzed by Pujals [29] and its composition is typical to metamorphosed zinc deposits. This testifies that Type 2a Pb-Zn mineralization is syn- to post-M_1 metamorphism. Alonso [32] demonstrated a predominant role of mechanical remobilization associated to deformation in the Bossòst anticlinorium and, especially, F_2 folds in Horcalh and fault in Liat. Our model is similar as we consider that the Variscan D_2 deformation locally remobilized Type 2a mineralization. The Margalida deposit records an additional deformational event compared to Victoria and Solitaria. Hosted in a ductile deformed marble and close to the Bossòst ductile fault, the Type 2a mineralization appears largely deformed with a typical durchbewegung texture. No sedimentary structure is recognized in the marble [70]. This attests for a Late Hercynian and/or Pyrenean deformation associated to the fault on the mineralization. Comparison with the Pierrefitte anticlinorium shows the same syn-D_1 Type 2a mineralization associated to regional thrust tectonics. The main exploited Pb-Zn mineralization in Pierrefitte mine was pluri-m scale levels parallel to S_0-S_1 and the regional thrust (Figure 10). Our work comforts the study of Nicol [60] which has shown an important remobilization of the mineralization in Ordovician and Devonian metasediments linked to D_1 deformation. On the contrary, Bois et al. [24] proposed a syngenetic deposition related to the activity of Late-Ordovician syn-sedimentary faults and volcanism that may have induced these mineralizations. In this case, remobilization is weak and sulfides crystalize prior to Variscan metamorphism [24]. But the presence of sphalerite parallel to S_1 cleavage and in pressure shadows around magnetite clast concordant to S_1 rather attests for a syn-D_1 mineralization event.

The third Type 2b vein mineralization (Figure 10) is parallel to S_2 cleavage. It intersects S_0-S_1 cleavage and former Type 2a stratabound mineralization. It has been recognized in the Pale Bidau-Argut-Pale de Rase districts [57] and Arre-Uzious-Anglas districts. It appears in a limited number of deposits in the PAZ. Type 2b mineralization is present in pluri-dm veins with restricted extension and highly differs structurally and mineralogically. The presence of Ge-minerals and absence of apatite, tourmaline, or

ilmenite are remarkable here. Nonetheless, possible Type 2a remobilization with external contribution is not excluded in the Type 2b vein formation. In the Uzious mine mineralization intersects magmatic aplite. Therefore it has probably emplaced syn- or post-Cauteret granite and is certainly late-Variscan in age (aplite from late-Variscan Cauteret granite) as supposed by Reyx [63]. Deformation of sphalerite, which is supposed to be syn-D_2 and/or syn-D_3, and the unusual sulfide paragenesis are inconsistent with a Mesozoic age as described in Aulus-Les Argentieres undeformed sphalerite [72]. Other Pb-Zn deposits, like the La Gela deposit [73] or Carboire deposit, could be attached to this third type as they are characterized by vertical Pb-Zn veins and presence of Ge-minerals. These late-Variscan Pb-Zn deposits have been recognized in Saint-Salvy (cf. M_2 mineralization) even if the main Pb-Zn mineralization event is Mesozoic [74].

6.2. Genetic Model of PAZ Pb-Zn Deposits Formation Linked to Regional Geology

The genetic model comprises four stages (Figure 11) based on the regional tectonic event model of Mezger and Passchier [22] and Garcia-Sansegundo and Alonso [56].

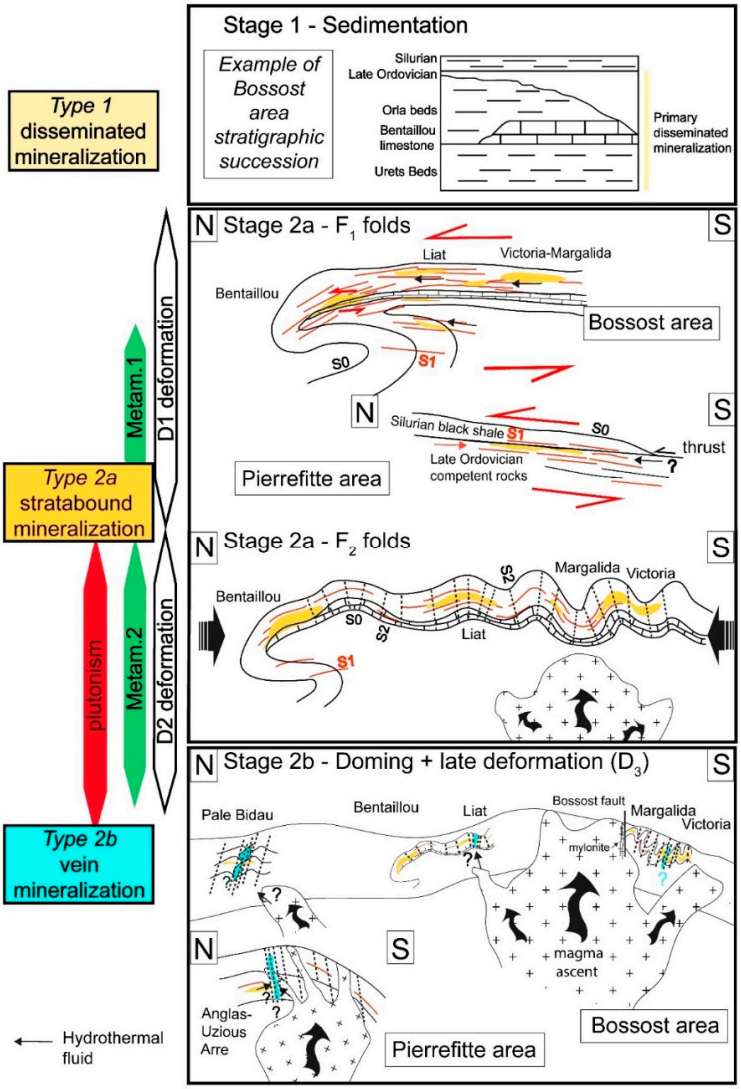

Figure 11. Genetic model for the formation of the three main Pb-Zn mineralization types. **Stage 1** is the disseminated Type 1 mineralization that is supposed to be syn-sedimentary. **Stage 2a** is the syn-D_1 Type 2a stratabound mineralization which is followed by the formation of F_2 folds and local remobilization of Pb-Zn mineralizations (saddle reef). **Stage 2b** represents the Type 2b late-Variscan vein mineralizations.

Stage 1 represents the syn-sedimentary layered mineralization (SEDEX deposit, Pb-Zn Type 1 disseminated mineralization). Primary sulfides were recognized in all pre-Silurian stratigraphic succession in the Bossòst area (Figure 11) and in Devonian rocks in Anglas-Uzious-Arre district. In the Pierrefitte area primary sphalerite is absent, which is probably linked to important hydrothermal low-grade alteration and D_1 overprint.

Stage 2a starts during the D_1 Variscan deformation and induces Type 2a stratabound mineralization. This mineralization occurs preferentially where a rheological contrast exists between two lithologies (e.g., marble-schist; schist-microconglomerates) and in highly D_1 deformed area (Figure 11). Stage 2a continues with D_2 Variscan deformation and the formation of N090–110°E F_2 upright folds. Granitic intrusions occur at that stage (Figure 11). This D_2 deformation locally reworked mineralization like in Victoria mines where the mineralization is remobilized in fold hinges. Horcalh mineralized fault [32] is interpreted as synchronous to D_2 deformation.

Stage 2b occurs during the doming phase and the late-Variscan Type 2b vein mineralizations (Figure 11). This mineralization type preferentially occurs parallel to the vertical S_2 cleavage and is mostly observed in the Pierrefitte and Bossòst anticlinoriums. Pull-apart-type structures are observed in Pale Bidau and Uzious mines. A late deformation D_3 corresponds to faults like the Bossòst mylonitic fault close to Margalida district.

We have shown that the Pb-Zn deposits in the PAZ were polyphased and closely linked to Variscan tectonics. There are at least three Pb-Zn mineralization-forming events, and two of them are evidently structurally controlled. Type 1 may be syngenetic, but little ore is present. The main exploited ores are Type 2a and Type 2b which have emplaced under a marked structurally control, either associated to S_1 and trapped in F_1 fold hinge, at lithology interface or in highly D_1 or D_2 deformed areas.

6.3. Is Pb-Zn Deposits Emplacement Sedimentary- or Structurally-Controlled?

SEDEX deposits are sedimentary controlled and syn- to diagenetic, and sulfides in them are laminated and included into the bedding [2]. In our study area, Pyrenean Pb-Zn mineralizations have been previously described as SEDEX by many authors [24,28–30,75,76]. The origin of several world-class Pb-Zn deposits is debated as well. For example, the geneses of Broken Hill-type deposit [6–12] or Jinding deposit [14–20] are still not understood and the authors have not yet decided between syngenetic or epigenetic models. In the Pyrenees, authors interpreted stratiform and lenses ore body shapes. The stratiform argument is not relevant because frequently S_0 stratification is parallel to the S_1 axial plane of isoclinal recumbent folds, typical of intensively deformed areas. Crystallization of sphalerite secant to isoclinal recumbent fold hinges attests that the main mineralization is parallel to S_1 and not to S_0. Structural observations are supported by the mineralogical study. The three PAZ Pb-Zn mineralization types contain the same constitutive minerals, like sphalerite, galena, and pyrite, but various trace minerals are present according to the type. These mineralogical differences are key parameters to distinguish between different Pb-Zn mineralization events in a single deposit.

In intensely deformed and metamorphosed terranes, the simple geometric link between mineralization and stratification is not relevant enough to distinguish between sedimentary or structural control. Structures are often parallelized due to pervasive tectonic events which makes the structural analysis difficult. Reworking of the ore-body during deformation can have obliterated geochemical tracers like isotopic data, especially Pb isotopes [77–79]. Consequently, a detailed structural study from regional to micro-scale focusing on the relationships between mineralization and cleavages is crucial. Pinpointing locations where structures like cleavage are secant (fold hinge), as well as deciphering textural relations between metamorphic minerals and mineralization, will lead to a better understanding of the ore-body genesis.

7. Conclusions

Three main types of Pb-Zn mineralizations have been distinguished in the Pyrenean Axial Zone. A minor type (Type 1) is a stratiform disseminated mineralization that presents syngenetic

characteristics. The two other mineralization types, previously described as SEDEX, are in reality post-sedimentation and formed as a result of Variscan polyphased tectonics: Type 2a is a syn-D_1 stratabound mineralization that is parallel to S_1 foliation. Type 2b is a syn to post-D_2 vein-type mineralization that is parallel to subvertical S_2 cleavage. Structural control is thus a key parameter for the remobilization of Pb-Zn mineralizations in this area like in (D_1 and D_2) fold hinges (saddle reef), high (D_1) deformed zones, rock contrast interfaces, and S_2 cleavages. A multiscale detailed structural study is essential for unraveling the formation of Pb-Zn deposits, especially in deformed and/or metamorphosed terranes.

Author Contributions: A.C. (Alexandre Cugerone) and B.C.-T. conceived the research within the framework of the A.C. (Alexandre Cugerone)'s PhD project; A.C. (Alexandre Cugerone), E.O., A.C. (Alain Chauvet), B.C.-T., J.G.B., and A.L. participated in field work; A.C. (Alexandre Cugerone) acquired the samples and performed all the analytical work under the guidance of A.C. (Alain Chauvet) and B.C.-T.; A.C. (Alexandre Cugerone) wrote the paper with contributions from E.O., B.C.-T., E.L.G., and J.G.B.

Funding: This research was funded by the French Geological Survey (Bureau de Recherches Géologiques et Minières; BRGM) through the national program "Référentiel Géologique de France" (RGF-Pyrénées).

Acknowledgments: The authors gratefully acknowledge Kalin Kouzmanov and Stefano Salvi for their involvement in the project. We thank the ARSHAL association for Bentaillou mine access and Jean-Marc Poudevigne, Louis de Pazzis, and Bernard Lafage for their precious knowledge of the Pyrenean Pb-Zn mines. We acknowledge Christophe Nevado and Doriane Delmas for thin section preparation. The authors are thankful for the editorial handling of Jax Jiang and for the constructive comments of the three anonymous reviewers.

Conflicts of Interest: The authors declare no conflicts of interest.

References

1. Wilkinson, J.J. Sediment-Hosted Zinc-Lead Mineralization: Processes and perspectives. *Treatise Geochem.* **2013**, *13*, 219–249.
2. Leach, D.L. Sediment-hosted lead-zinc deposits: A global perspective. *Econ. Geol.* **2005**, *100*, 561–607.
3. Moore, D.W.; Young, L.E.; Modene, J.S.; Plahuta, J.T. Geologic setting and genesis of the Red Dog zinc-lead-silver deposit, western Brooks Range, Alaska. *Econ. Geol.* **1986**, *81*, 1696–1727. [CrossRef]
4. Kelley, K.D.; Jennings, S. A special issue devoted to barite and Zn-Pb-Ag deposits in the Red Dog district, Western Brooks Range, northern Alaska. *Econ. Geol.* **2004**, *99*, 1267–1280. [CrossRef]
5. Hazarika, P.; Upadhyay, D.; Mishra, B. Contrasting geochronological evolution of the Rajpura-Dariba and Rampura-Agucha metamorphosed Zn-Pb deposit, Aravalli-Delhi Belt, India. *J. Asian Earth Sci.* **2013**, *73*, 429–439. [CrossRef]
6. Lawrence, L.J. Polymetamorphism of the sulphide ores of Broken Hill, NSW, Australia. *Miner. Depos.* **1973**, *8*, 211–236. [CrossRef]
7. Gibson, G.M.; Nutman, A.P. Detachment faulting and bimodal magmatism in the Palaeoproterozoic Willyama Supergroup, south-central Australia; keys to recognition of a multiply deformed Precambrian metamorphic core complex. *J. Geol. Soc.* **2004**, *161*, 55–66. [CrossRef]
8. Hobbs, B.E.; Walshe, J.L.; Ord, A.; Zhang, Y.; Carr, G.C. The Broken Hill orebody: A high temperature, high pressure scenario. *AGSO Rec.* **1998**, *2*, 98–103.
9. Walters, S.; Bailey, A. Geology and mineralization of the Cannington Ag-Pb-Zn deposit: An example of Broken Hill-Type mineralization in the eastern succession, Mount Isa Inlier, Australia. *Econ. Geol.* **1998**, *93*, 1307–1329. [CrossRef]
10. Webster, A.E. The Structural Evolution of the Broken Hill Pb-Zn-Ag Deposit, New South Wales, Australia. Ph.D. Thesis, University of Tasmania, Hobart, Australia, 2004.
11. Bodon, S.B. Paragenetic relationships and their implications for ore genesis at the Cannington Ag-Pb-Zn deposit, Mount Isa inlier, Queensland, Australia. *Econ. Geol.* **1998**, *93*, 1463–1488. [CrossRef]
12. Haydon, R.C.; Mcconachy, G.W. The stratigraphic setting of Pb-Zn-Ag mineralization at Broken Hill. *Econ. Geol.* **1987**, *82*, 826–856. [CrossRef]
13. Yalikun, Y.; Xue, C.; Symons, D.T.A. Paleomagnetic age and tectonic constraints on the genesis of the giant Jinding Zn-Pb deposit, Yunnan, China. *Miner. Depos.* **2018**, *53*, 245–259. [CrossRef]

14. Shi, J.X.; Yi, F.H.; Wen, Q.D. The rock-ore characteristics and mineralisation of Jinding lead-zinc deposit, Lanping. *J. Yunnan Geol.* **1983**, *2*, 179–195.
15. Wang, J.B.; Li, C.Y.; Chen, X. A new genetic model for the Jinding lead-zinc deposit. *Geol. Explor. Non Ferr. Met.* **1992**, *1*, 200–206. (In Chinese)
16. Leach, D.L.; Song, Y.C.; Hou, Z.Q. The world-class Jinding Zn–Pb deposit: Ore formation in an evaporite dome, Lanping Basin, Yunnan, China. *Miner. Depos.* **2017**, *52*, 281–296. [CrossRef]
17. Kyle, J.R.; Li, N. Jinding: A giant tertiary sandstone-hosted Zn–Pb deposit, Yunnan, China. *SEG Newsl.* **2002**, *50*, 1–9.
18. Chi, G.; Xue, C.; Qing, H.; Xue, W.; Zhang, J.; Sun, Y. Hydrodynamic analysis of clastic injection and hydraulic fracturing structures in the Jinding Zn-Pb deposit, Yunnan, China. *Geosci. Front.* **2012**, *3*, 73–84. [CrossRef]
19. Xue, C.; Zeng, R.; Liu, S.; Chi, G.; Qing, H.; Chen, Y.; Yang, J.; Wang, D. Geologic, fluid inclusion and isotopic characteristics of the Jinding Zn-Pb deposit, western Yunnan, South China: A review. *Ore Geol. Rev.* **2007**, *31*, 337–359. [CrossRef]
20. Chi, G.; Qing, H.; Xue, C. An overpressured fluid system associated with the giant sandstone-hosted Jinding Zn-Pb deposit, western Yunnan, China Chapter. In *Mineral Deposit Research: Meeting the Global Challenge*; Mao, J., Bierlein, F.P., Eds.; Springer: Berlin, German, 2005; pp. 93–96.
21. Zwart, H.J. The Geology of the Central Pyrenees. *Leidse Geol. Meded.* **1979**, *50*, 1–74.
22. Mezger, J.E.; Passchier, C.W. Polymetamorphism and ductile deformation of staurolite-cordierite schist of the Bossòst dome: Indication for Variscan extension in the Axial Zone of the central Pyrenees. *Geol. Mag.* **2003**, *140*, 595–612. [CrossRef]
23. Denèle, Y.; Laumonier, B.; Paquette, J.-L.; Olivier, P.; Gleizes, G.; Barbey, P. Timing of granite emplacement, crustal flow and gneiss dome formation in the Variscan segment of the Pyrenees. *Geol. Soc. Lond. Spec. Publ.* **2014**, *405*, 265–287. [CrossRef]
24. Bois, J.P.; Pouit, G. Les minéralisations de Zn (Pb) de l'anticlinorium de Pierrefitte: Un exemple de gisements hydrothermaux et sédimentaires associés au volcanisme dans le Paléozoïque des Pyrénées centrales. *Bureau Rech. Geol. Min.* **1976**, *6*, 543–567. (In French)
25. Pouit, G.; Fortuné, J.-P. Métallogénie comparée des Pyrénées et du Sud du Massif-central. In Proceedings of the 26ème Congrès Géologique International, Paris, France, 7–17 July 1980; p. 61. (In French)
26. Fert, D. Un Aspect de la Métallogénie du Zinc et du Plomb Dans l'Ordovicien des Pyrénées Centrales: Le District de Sentein (Ariège, Haute-Garonne). Ph.D. Thesis, University Pierre Marie Curie, Paris, France, 1976.
27. Pouit, G. Différents Modèles de Mineralisations «Hydrothermale Sédimentaire», à Zn (Pb) du Paléozoïque des Pyrénees Centrales. *Miner. Depos.* **1978**, *13*, 411–421. (In French) [CrossRef]
28. Pouit, G. Les minéralisations Zn-Pb exhalatives sédimentaires de Bentaillou et de l'anticlinorium paléozoïque de Bosost (Pyrénées ariégeoises, France). *Chron. Rech. Min.* **1986**, *485*, 3–16. (In French)
29. Pujals, I. Las Mineralizaciones de Sulfuros en el Cambro-Ordovicico de la Val d'Aran (Pirineo Central, Lérida). Ph.D. Thesis, University Autónoma Barcelona, Barcelona, Spain, 1992.
30. Cardellach, E.; Phillips, R.; Ayora, C. Metamorphosed stratiform sulphides of the Liat area, Central Pyrenees, Spain. *Inst. Min. Metall. Trans.* **1982**, *91*, 90–95. (In Spanish)
31. Cardellach, E. Estudio microscópico de las mineralizaciones de Pb-Zn de Liat, Baguergue y Montoliu. *Acta Geol. Hisp.* **1977**, *12*, 120–122. (In Spanish)
32. Alonso, J.L. Deformaciones Sucesivas en el Area Comprendida Entre Liat y el Puerto de Orla—Control Estructural de los Depositos de Sulfuros (Valle de Aran, Pirineos Centrales). Master's Thesis, University Oviedo, Oviedo, Spain, 1979. (In Spanish)
33. Nicol, N. Etude Structurale des Minéralisations Zn-Pb du Paléozoïque du Dôme de Pierrefitte (Hautes-Pyrénées). Goniométrie de Texture Appliquée aux Minéraux Transparents et Opaques. Ph.D. Thesis, University Orléans, Orléans, France, 1997. (In French)
34. García-Sansegundo, J.; Martin-Izard, A.; Gavaldà, J. Structural control and geological significance of the Zn-Pb ores formed in the Benasque Pass area (Central Pyrenees) during the post-late Ordovician extensional event of the Gondwana margin. *Ore Geol. Rev.* **2014**, *56*, 516–527. [CrossRef]
35. Marcoux, E. Isotope du plomb et paragénèses métalliques, traceurs de l'histoire des gites mineraux. *Bur. Rech. Geol. Min.* **1986**, *117*, 1–289. (In French)
36. Zwart, H.J. Metamorphic history of the Central Pyrenees, Part II, Valle de Aran. *Leidse Geol. Meded.* **1963**, *28*, 321–376.

37. Kleinsmiede, W.F.J. Geology of the Valle de Aran (Central Pyrenees). *Leidse Geol. Meded.* **1960**, *25*, 129–245.
38. Cochelin, B.; Lemirre, B.; Denèle, Y.; De Saint Blanquat, M.; Lahfid, A.; Duchêne, S. Structural inheritance in the Central Pyrenees: The Variscan to Alpine tectonometamorphic evolution of the Axial Zone. *J. Geol. Soc. Lond.* **2017**, *175*, 16. [CrossRef]
39. De Sitter, L.U.; Zwart, H.J. Tectonic development in supra and infra-structures of a mountain chain. In *Structure of the Earth's Crust and Deformation of Rocks*; Det Berlingske Bogtrykkeri: Copenhagen, Denmark, 1960; Volume 18, pp. 248–256.
40. Carreras, J.; Capellà, I. Tectonic levels in the Palaeozoic basement of the Pyrenees: A review and a new interpretation. *J. Struct. Geol.* **1994**, *16*, 1509–1524. [CrossRef]
41. Carreras, J.; Druguet, E. Framing the tectonic regime of the NE Iberian Variscan segment. *Geol. Soc. Lond. Spec. Publ.* **2014**, *405*, 249–264. [CrossRef]
42. Cochelin, B. Champ de déformation du socle Paléozoïque des Pyrénées. Ph.D. Thesis, Université Toulouse 3 Paul Sabatier, Toulouse, France, 2016. (In French)
43. Mezger, J.E.; Gerdes, A. Early Variscan (Visean) granites in the core of central Pyrenean gneiss domes: Implications from laser ablation U-Pb and Th-Pb studies. *Gondwana Res.* **2016**, *29*, 181–198. [CrossRef]
44. Pouget, P. Hercynian tectonometamorphic evolution of the Bosost dome (French Spanish Central Pyrenees). *J. Geol. Soc. Lond.* **1991**, *148*, 299–314. [CrossRef]
45. Mezger, J.E. Comparison of the western Aston-Hospitalet and the Bossòst domes: Evidence for polymetamorphism and its implications for the Variscan tectonic evolution of the Axial Zone of the Pyrenees. *J. Virtual Explor.* **2005**, *19*, 1–19. [CrossRef]
46. Mezger, J.E.; Schnapperelle, S.; Rölke, C. Evolution of the Central Pyrenean Mérens fault controlled by near collision of two gneiss domes. *Hallesches Jahrb.* **2012**, *34*, 11–29.
47. Carreras, J. Zooming on Northern Cap de Creus shear zones. *J. Struct. Geol.* **2001**, *23*, 1457–1486. [CrossRef]
48. *BRGM International Report: Les Gisements de Pb-Zn Français (Situation en 1977)*; BRGM: Orléans, France, 1984; pp. 1–278. (In French)
49. Ovejero Zappino, G. Mineralizaciones Zn-Pb ordovícicas del anticlinorio de Bossost. Yacimientos de Liat y Victoria. Valle de Arán. Pirineo (España). *Bol. Geol. Min.* **1991**, *102*, 356–377. (In Spanish)
50. Castroviejo Bolibar, R.; Serrano, F.M. Estructura y metalogenia del campo filoniano de Cierco (Pb-Zn-Ag), en el Pirineo de Lérida. *Bol. Geol. Min.* **1983**, *1983*, 291–320. (In Spanish)
51. Aerden, D.G.A. Kinematics of orogenic collapse in the Variscan Pyrenees deduced from microstructures in porphyroblastic rocks from the Lys-Caillaouas massif. *Tectonophysics* **1994**, *238*, 139–160. [CrossRef]
52. Barrère, P.; Bouquet, C.; Debroas, E.J.; Pelissonnier, H.; Peybernes, B.; Soulé, J.C.; Souquet, P.; Ternet, Y. Arreau. In *BRGM Geological Map 1/50,000 with Note*; BRGM: Orléans, France, 1984; p. 60. (In French)
53. Clin, M.; Taillefer, F.; Pouchan, P.; Muller, A. Bagnères de Luchon. In *BRGM Geological Map 1/50,000 with Note*; BRGM: Orléans, France, 1989; p. 78. (In French)
54. Lavigne, J. Pic de Mauberme. In *BRGM Geological Map 1/50,000 with Note*; BRGM: Orléans, France, 1972; p. 24. (In French)
55. García-Sansegundo, J.; Merino, J.R.; Santisteban, R.R.; Leyva, F. Canejan-Vielha Mapa geologico 1:50,000. *Inst. Geol. Min. Espana* **2013**, *1*, 66. (In French)
56. Garcia-Sansegundo, J.; Alonso, J.L. Stratigraphy and structure of the southeastern Garona Dome. *Geodin. Acta* **1989**, *3*, 127–134. [CrossRef]
57. Cugerone, A.; Cenki-Tok, B.; Chauvet, A.; Le Goff, E.; Bailly, L.; Alard, O.; Allard, M. Relationships between the occurrence of accessory Ge-minerals and sphalerite in Variscan Pb-Zn deposits of the Bossost anticlinorium, French Pyrenean Axial Zone: Chemistry, microstructures and ore-deposit setting. *Ore Geol. Rev.* **2018**, *95*, 1–19. [CrossRef]
58. Dubois, C. *Mangeuses d'homme: L'épopée des Mines de Bentaillou et de Bulard en Ariège*; Privat Edition: Toulouse, France, 2015; p. 320. (In French)
59. Barrère, P.; Bois, J.-P.; Soulé, J.-C.; Ternet, Y. Argelès-Gazost. In *BRGM Geological Map 1/50,000 with Note*; BRGM: Orléans, France, 1980; pp. 1–48. (In French)
60. Nicol, N.; Legendre, O.; Charvet, J. Les minéralisations Zn-Pb de la série paléozoïque de Pierrefitte (Hautes-Pyrénées) dans la succession des évènements tectoniques hercyniens. *C. R. Acad. Sci.* **1997**, *324*, 453–460. (In French)

61. Calvet, P. Etude Structurale et Métallogénique de L'anticlinorium de Pierrefitte: Influence de la Déformation sur les Minéralisations Stratiformes. Ph.D. Thesis, University d'Orléans, Orléans, France, 1988; p. 283. (In French)
62. Alvarez-Perez, A.; Campa-Vineta, J.A.; Montoriol-Pous, J. Sobre la presencia de gahnita ferrífera en Bossost (Vall D'Aran, Lérida). *Acta Geol. Hisp.* **1974**, *9*, 111–113. (In Spanish)
63. Reyx, J. Relations entre Tectonique, Métamorphisme de Contact et Concentrations Metalliques dans le Secteur des Anciennes Mines d'Arre et Anglas (Hautes-Pyrénées-Pyrénées atlantiques). Ph.D. Thesis, University Paris VI, Paris, France, 1973; p. 83. (In French)
64. Scott, R.J.; Meffre, S.; Woodhead, J.; Gilbert, S.E.; Berry, R.F.; Emsbo, P. Development of framboidal pyrite during diagenesis, low-grade regional metamorphism, and hydrothermal alteration. *Econ. Geol.* **2009**, *104*, 1143–1168. [CrossRef]
65. Vernhet, Y. Les Minéralisations Zincifères de l'Ordovicien et du Dévonien du Val d'Orle (District de Sentein, Ariège) et de la région de Fourcaye (Val d'Aran, Espagne). Ph.D. Thesis, University Pierre Marie Curie, Paris, France, 1981; p. 279. (In French)
66. Windh, J. Saddle Reef and Related Gold Mineralization, Hill End Gold Field, Australia: Evolution of an Auriferous Vein System during Progressive Deformation. *Econ. Geol.* **1995**, *90*, 1764–1775. [CrossRef]
67. Bull, S.W.; Large, R.R. Setting the stage for the genesis of the giant Bendigo ore system. *Geol. Soc. Lond. Spec. Publ.* **2015**, *393*, 161–187. [CrossRef]
68. Zeng, M.; Zhang, D.; Zhang, Z.; Li, T.; Li, C.; Wei, C. Structural controls on the Lala iron-copper deposit of the Kangdian metallogenic province, southwestern China: Tectonic and metallogenic implications. *Ore Geol. Rev.* **2018**, *97*, 35–54. [CrossRef]
69. Cardellach, E.; Alvarez-Perez, A. Interpretación genética de las mineralizaciones de Pb-Zn del Ordovícico Sup. de la Vall de Aran. *Acta Geol. Hisp.* **1979**, *14*, 117–120. (In Spanish)
70. Alvarez-Perez, A.; Campa-Vineta, J.A.; Montoriol-Pous, J. Mineralogénesis de los yacimientos del área de Bossost (Vall d'Aran, Lérida). *Acta Geol. Hisp.* **1977**, *4–6*, 123–126. (In Spanish)
71. Ovejero Zappino, G. Mineralizaciones Zn-Pb del Ordovicico Superior del Valle de Aran (Anticlinorio de Bossost). Pireneo de Lerida (Espana). *Bol. Soc. Esp. Mineral.* **1987**, *10*, 35–37.
72. Munoz, M.; Baron, S.; Boucher, A.; Béziat, D.; Salvi, S. Mesozoic vein-type Pb-Zn mineralization in the Pyrenees: Lead isotopic and fluid inclusion evidence from the Les Argentières and Lacore deposits. *C. R. Geosci.* **2015**, *348*, 322–332. [CrossRef]
73. Militon, C. Métallogénie polyphasée à Zn, Pb, Ba, F et Mg, Fe de ma région de Gèdre-Gavarnie-Barroude (Hautes-Pyrénées). Ph.D. Thesis, University d'Orléans, Orléans, France, 1987. (In French)
74. Munoz, M.; Boyce, A.J.; Courjault-Rade, P.; Fallick, A.E.; Tollon, F. Multi-stage fluid incursion in the Palaeozoic basement-hosted Saint-Salvy ore deposit (NW Montagne Noire, southern France). *Appl. Geochem.* **1994**, *9*, 609–626. [CrossRef]
75. Pouit, G. Les minéralisations Zn-Pb dans l'Ordovicien des Pyrénées centrales-Etude préliminaire. *Rapp. BRGM* **1974**, *74*, 50. (In French)
76. Pouit, G.; Bois, J.P. Arrens Zn (Pb), Ba Devonian deposit, Pyrénées, France: An exhalative-sedimentary-type deposit similar to Meggen. *Miner. Depos.* **1986**, *21*, 181–189. [CrossRef]
77. Wagner, T.; Schneider, J. Lead isotope systematics of vein-type antimony mineralization, Rheinisches Schiefergebirge, Germany: A case history of complex reaction and remobilization processes. *Miner. Depos.* **2002**, *37*, 185–197. [CrossRef]
78. Marcoux, E.; Moelo, Y. Lead isotope geochemistry and paragenetic study of inheritance phenomena in metallogenesis: Examples from base metal sulfide deposits in France. *Econ. Geol.* **1991**, *86*, 106–120. [CrossRef]
79. Kamona, A.F.; Lévêque, J.; Friedrich, G.; Haack, U. Lead isotopes of the carbonate-hosted Kabwe, Tsumeb, and Kipushi Pb-Zn-Cu sulphide deposits in relation to Pan African orogenesis in the Damaran-Lufilian Fold Belt of Central Africa. *Miner. Depos.* **1999**, *34*, 273–283. [CrossRef]